Interactive Phenomena in Supersonic Jet Mixing Problems, Part I: Phenomenology and Numerical Modeling Techniques

Sanford M. Dash* and David E. Wolf†
Science Applications Inc., Princeton, New Jersey

The interactive phenomena that occur in supersonic jet mixing flowfields, and numerical modeling techniques developed to analyze such phenomena are discussed. A spatial marching procedure based on solving the parabolized Navier-Stokes jet mixing equations is presented. This procedure combines shock-capturing methodology for the analysis of supersonic mixing regions with pressure-split methodology for the analysis of subsonic mixing regions. The two regions are coupled at viscous sonic lines utilizing a viscous-characteristic coupling procedure. Specialized techniques for the treatment of jet boundary growth, strong discontinuities (Mach disks), and small embedded subsonic zones (behind Mach disks) are presented. Turbulent processes are represented by two-equation turbulence model formulations. In Part II of this article, numerical studies are presented for a variety of supersonic jet interactive phenomena.

Introduction

THE analysis of the plume flowfield generated by the interaction of an imperfectly expanded supersonic jet with its surrounding environment involves consideration of a number of distinct flow regions with varying characteristic features and length scales. The jet near field (Fig. 1) is characterized by a predominantly inviscid shock cell structure with thin shear layers developing along the plume and Mach disk slipstreams. Embedded zones of subsonic flow occur behind Mach disks, while a significant portion of the plume mixing layer will be subsonic for jets exhausting into subsonic external streams. A transitional region (Fig. 2) joins the predominantly inviscid near field with the fully viscous, pressure-equilibrated far field. Here, the mixing layers come to engulf the entire jet and wave processes occur in a strongly turbulent environment. In this region, wave fronts are curved by the flow rotationality and wave intensities are diminished by turbulent dissipative effects. In the jet far field, wave processes have been totally dissipated and classical parabolic (constant pressure) mixing prevails.

Practical solutions of interactive supersonic jet flowfields have been achieved via the use of patched zonal techniques that employ separate integration components to analyze the various regions of the plume. Models utilizing this technique recently have been developed by Dash et al.[1-5] for the near-field analysis of two-dimensional aircraft and rocket plume flowfields where a weakly interactive overlaid coupling approach[6] often can be justified. However, these models cannot deal with strongly interactive near-field phenomena such as:

1) Shock/compression waves produced by the positive displacement effect of rapid chemistry or high Mach number viscous dissipation in the plume shear layer.

2) Strong expansion waves generated by the "washing away" of large mass defect initial regions downstream of base/separated flow zones.

3) The negative displacement of streamlines downstream of Mach disks generated by the wake-like entrainment process.

4) The shock/shear layer interactions occurring at the end of near-field shock cells for situations where a significant portion of the near-field jet core has been entrained into the jet shear layer.

Some of the preceding interactive phenomena are schematized in Fig. 3.

The transitional region (Fig. 2), where wave processes are largely embedded in the turbulent mixing layer, is always a region of strong viscous/inviscid interactions and cannot be treated by weakly interactive overlaid methodology. The damping of wave amplitudes occurring in this region is schematized in Fig. 2. For many engineering applications (i.e., rocket plume signature prediction[7] or vehicle design, and for aircraft plume/afterbody interaction problems[8]), the decaying wave structure in the transitional region has a negligible influence on the solution. For the analysis of jet

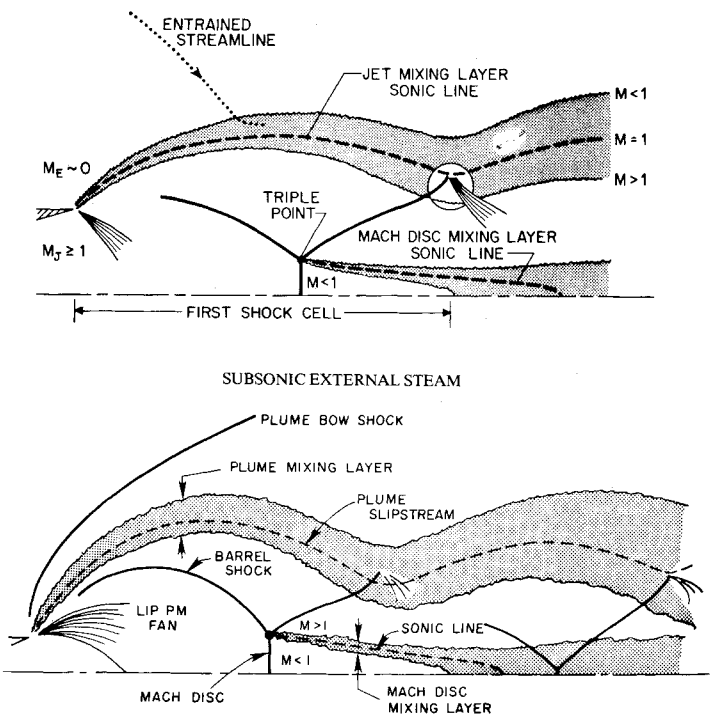

Fig. 1 Schematic of jet near field structure for supersonic and subsonic external flows.

Presented as part of Paper 83-0288 at the AIAA 21st Aerospace Sciences Meeting, Reno, Nev., Jan 10-13, 1983; submitted Jan. 29, 1983; revision submitted Aug. 24, 1983. Copyright © American Institute of Aeronautics and Astronautics, Inc., 1983. All rights reserved.

*Technical Director, Propulsion Gas Dynamics Division. Member AIAA.

†Research Scientist, Propulsion Gas Dynamics Division. Member AIAA.

laboratory data or for applications to problem areas such as jet shock noise,[9] the details of the shock structure in this transitional region are quite important.

Aside from the inability of "overlaid" zonal models to treat strongly interactive near-field phenomena adequately, and to analyze the jet transitional region, the extension of these models to the analysis of three-dimensional jet flowfields is not at all straightforward. The interpolations entailed become cumbersome, the inviscid map storage requirements become excessive, and the use of displacement-thickness concepts to define the effective jet geometry[10] break down due to the highly nonuniform cross-flow pressure fields that can occur in three dimensions. To analyze strongly interactive jet flowfields in both two- and three-dimensional situations, computational procedures are required that 1) intimately couple viscous and inviscid flow processes in the jet mixing regions, and 2) utilize strongly interactive coupling techniques to couple the viscous/inviscid jet and external flow solutions. This article will describe extensions of the present zonal models to achieve these requirements.

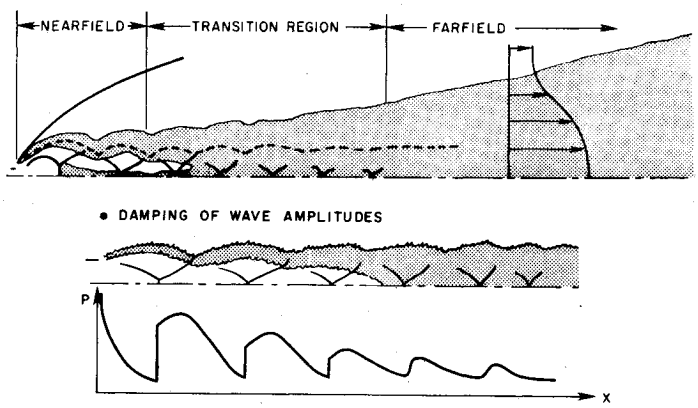

Fig. 2 Schematic of jet near field, far field, and transitional regions; damping of wave amplitudes by turbulence in transitional region.

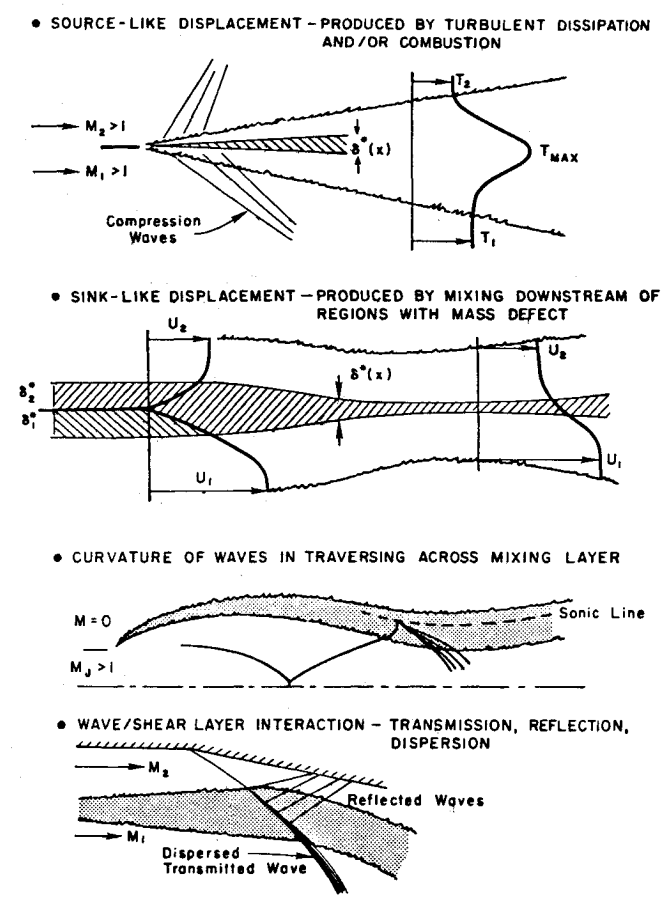

Fig. 3 Fundamental interactive phenomena occurring in supersonic mixing flowfields.

The overall objectives of this work are multifaceted and include the following specific goals:

1) The development of computational procedures for the analysis of strongly interactive jet mixing phenomena in two-dimensions.

2) The development of a computer code that utilizes these procedures to calculate the coupled multiple-cell shock structure and turbulent mixing in "simple," imperfectly expanded two-dimensional jets for aircraft shock-noise applications.

3) The extension of this code to analyze "complex" (chemically reacting, multiphase, multicomponent, gas/particle mixtures) two-dimensional jets for rocket plume applications.

4) The formulation of new coupling procedures for jet/subsonic-transonic flowfield interactions via extensions of present interactive boundary-layer concepts.

5) The extension of the two-dimensional computational procedures to three-dimensional jet flowfields.

6) The development of a computer code to predict a variety of three-dimensional interactive jet flowfield problems.

This article will focus upon the first of these goals. Procedures for analyzing two-dimensional interactive jet phenomena are discussed based on fully coupled solutions of the parabolized Navier-Stokes (PNS) jet mixing equations. The hyperbolic, inviscid shock-capturing component, SCIPPY,[11] of the overlaid zonal models has been extended to integrate the PNS equations in supersonic jet mixing regions. Spatial marching in subsonic regions is accomplished via a pressure-splitting approximation[12] and the two solutions are coupled at the viscous jet and Mach disk mixing layer sonic lines utilizing a viscous-characteristic coupling technique.[13] Previous PNS jet solutions have either been restricted to fully supersonic flows[14,15] or have utilized "wave-solving" extensions[16,17] of pressure-split, partially parabolic algorithms[12] which cannot treat the strong, entropy-producing shock waves encountered in significantly underexpanded jets. A review of the PNS jet solutions is given in Ref. 18. The present approach *combines* supersonic strong shock-capturing methodology and subsonic pressure-split methodology in the framework of a single numerical model and thus represents a substantial improvement over existing models. In Part II of this article,[43] applications of this new model to a variety of supersonic jet mixing interactive phenomena will be exhibited.

The second of the above itemized goals has been met by the development of the SCIPVIS computer code[19] which has been catered specifically for useage in jet shock-noise applications.[20] The ability of this code to predict the decaying wave structure accurately in both over- and underexpanded simple laboratory jets has been demonstrated via comparisons of predictions with data for Mach 1, 1.5, and 2 jets exhausting into still air at various pressure ratios.[20] The sensitivity of these calculations to the turbulence model formulation utilized, and, in particular, to the models' representation of high Mach number compressibility effects, is presented in Ref. 19. The extension of SCIPVIS methodology to "complex" jet flowfields as occur in rocket plumes is described in Refs. 21 and 22. Coupling procedures for jet/subsonic-transonic flow interactions based on the direct coupling methodology of Mahgoub and Bradshaw[23] and on the velocity-split coupling approach of Khosla and Rubin[24] have been formulated as described in Refs. 5 and 25. A preliminary three-dimensional version of SCIPVIS is now operational for supersonic mixing problems and will be described in a forthcoming publication.[44]

Governing Equations

Mean Flow Equations

The commonly employed PNS equations governing the planar ($J=0$) or axisymmetric ($J=1$) turbulent mixing of a high Reynolds number moderately under- (or over-) expanded jet are given below.

$$\frac{\partial \bar{E}}{\partial x}+\frac{\partial \bar{F}}{\partial r}+\left(\bar{G}_f+\frac{J\bar{F}}{r}\right)=\frac{1}{r^J}\frac{\partial}{\partial r}\left(\frac{r^J\mu_t}{\sigma_f}\frac{\partial \bar{f}}{\partial r}\right) \tag{1}$$

where

$$\bar{E}=\begin{bmatrix} e_\rho \\ e_u \\ e_v \\ e_H \\ e_\phi \end{bmatrix}=\begin{bmatrix} \rho U \\ P+\rho U^2 \\ \rho UV \\ \rho UH \\ \rho U\phi \end{bmatrix}$$

$$\bar{F}=\begin{bmatrix} \rho V \\ \rho UV \\ P+\rho V^2 \\ \rho VH \\ \rho V\phi \end{bmatrix}, \quad \bar{f}=\begin{bmatrix} 1 \\ U \\ V \\ H \\ \phi \end{bmatrix}$$

and the source terms G_f are zero for the continuity, momentum, and species diffusion (ϕ) equations. The source term G_H for the energy equation is given by

$$G_H=-\frac{1}{r^J}\frac{\partial}{\partial r}\left[r^J\frac{\mu_t}{\sigma_H}(\sigma_{H-1})\frac{\partial}{\partial r}\left(\frac{U^2}{2}\right)\right] \tag{2}$$

In the above equations, U and V are the axial and radial velocity components, P the pressure, ρ the density, H the total enthalpy, ϕ a species parameter, μ_t the turbulent viscosity, and σ_f the "effective" Prandtl number for each variable defined below

$$\sigma_f^{-1}=[1,1,\tfrac{3}{4},Pr_t,Pr_t]^T \tag{3}$$

under the assumption that the turbulent transport of heat and mass are the same (i.e., $\sigma_H=\sigma_\phi=Pr_t$).

The mixing problems to be discussed here assume that the jet and external streams are each of uniform composition and the chemistry is frozen. Thus, the local composition, α_i, can be defined by the single species parameter ϕ via the relation:

$$\alpha_i=\alpha_{iE}+\phi(\alpha_{iJ}-\alpha_{iE}) \tag{4}$$

where α_i is the mass fraction of the ith species and J and E designate the constant values of α_i in the unmixed jet and external streams. Thus ϕ varies from 1 to 0 in traversing the jet shear layer until the mixing reaches the axis. The local molecular weight in the jet mixing layer is a simple function of ϕ and the molecular weights of the unmixed streams, while the static enthalpy h, specific heat Cp, and specific heat ratio γ, are functions of ϕ and temperature (see Ref. 26 for the expressions utilized).

Turbulence Models

A number of two-equation turbulence models have been utilized in this study which include: 1) the $k\epsilon 1$ and $k\epsilon 2$ models of Launder et al.[27]; 2) compressibility corrected versions of these models[28]; and 3) a compressibility corrected version[29] of the Spalding kW model.[30]

The performance of these models for aircraft and rocket plume applications recently has been assessed by Pergament[31] utilizing a large body of available jet data. A new assessment study is now in progress utilizing the supersonic jet data recently obtained at Calspan.[32] These assessment studies clearly have exhibited the inability of standard "incompressible" turbulence models[27,30] to predict appropriate mixing rates for supersonic free mixing problems. Present-generation compressibility corrected models[28,29] have been formulated utilizing heuristic considerations and their overall reliability for "complex" mixing problems remains questionable. An assessment of the performance of these models for supersonic underexpanded jets utilizing the detailed static pressure measurements of Seiner and Norum[9] is presented in Refs. 19 and 20. A marked sensitivity of the jet shock structure to the turbulence model employed has been exhibited. Fortuitously, the compressibility corrected models that performed best for simple, perfectly expanded supersonic jet mixing problems[31] have performed comparably in a complex pressure environment.

A detailed description of these turbulence models, as incorporated into this PNS jet model, is available in Ref. 19. For the purpose of this article, the following brief descriptions of these models are provided for clarity. The $k\epsilon$ turbulence models relate the turbulent viscosity μ_t to the turbulent kinetic energy k and dissipation rate ϵ via the relation:

$$\mu_t=\rho K(M_\tau)C_\mu(f,g)\frac{k^2}{\epsilon} \tag{5}$$

where $K(M_\tau)$ is the compressibility correction coefficient[28] (M_τ is the local Mach number of the turbulence fluctuations as given by $k^{1/2}/a$) and $C_\mu(f,g)$ is the turbulent viscosity coefficient[27] (f and g are axisymmetric and weak-shear parameters). The partial differential equations for k and ϵ take the form of Eq. (1) with the source terms given by

$$-G_k=\underline{P}-\rho\epsilon \tag{6a}$$

$$-G_\epsilon=(C_1\underline{P}-C_2\rho\epsilon)\frac{\epsilon}{k} \tag{6b}$$

where

$$\underline{P}=\mu_t\left(\frac{\partial U}{\partial r}\right)^2$$

The kW turbulence model relates the turbulent viscosity to the turbulent kinetic energy and vorticity fluctuation parameter W via the relation

$$\mu_t=\rho k/W^{1/2} \tag{7}$$

The partial differential equations for k and W take the form of Eq. (1) with source terms given by

$$-G_k=\underline{P}-\rho C_D kW^{1/2} \tag{8a}$$

$$-G_W=\frac{C_1W\underline{P}-C_2\rho kW^{3/2}}{k}+C_3\mu_t\left(\frac{\partial^2 U}{\partial r^2}\right)^2 \tag{8b}$$

The specific coefficients and effective Prandtl numbers utilized in implementing these turbulence models are provided in Ref. 19.

Mapped Conservation Equations

The system of mean flow and turbulence model equations is solved in a mapped rectangular domain utilizing the trans-

formation:

$$\xi = x$$

$$\eta = (r - r_L(x))/(r_U(x) - r_L(x)) \tag{9}$$

where r_L and r_U are the lower and upper boundaries of the domain being solved. With this transformation, the equations can be expressed in the following vector form:

$$\boxed{\frac{\partial E}{\partial \xi} + \frac{\partial F}{\partial \eta} = \frac{b^2}{r^J}\frac{\partial}{\partial \eta}\left(\frac{r^J \mu_t}{\sigma_f}\frac{\partial f}{\partial \eta}\right) - G_f} \tag{10}$$

where f and E are equivalent to the arrays of Eq. (1) extended by the turbulence model variables

$$F = b\bar{F} - a\bar{E}$$

and

$$G_f = \bar{G}_f + \frac{J\bar{F}}{r} + a_\eta \bar{E}$$

[with $\bar{E}$ and $\bar{F}$ defined in Eq. (1) and the nonzero source terms G_H, G_k, G_ϵ, and G_W defined in Eqs. (2), (6), and (8)]. In the above equations, the mapping transformation parameters a and b are defined by

$$a(\xi,\eta) = (1-\eta)r_L' + \eta r_U'/(r_U - r_L)$$

$$b(\xi) = 1/(r_U - r_L) \tag{11}$$

Viscous-Characteristic Equations

Characteristic relations are utilized at supersonic boundary points and in the vicinity of the viscous sonic lines that occur in the jet and Mach disk mixing layers (Fig. 1) to aid in the coupling of the subsonic and supersonic regions of the jet. In turbulent mixing regions, the diffusion terms are included in the characteristic relations as local source terms following the procedure of Ref. 13. Along the $\lambda^\pm$ characteristic directions defined by

$$\lambda^\pm = \frac{dr^\pm}{dx} = \tan(\theta \pm \mu) \tag{12}$$

the following viscous-characteristic pressure/flow deflection angle (θ) compatibility relation applies:

$$\frac{\sin\mu\cos\mu}{\gamma}\, d\ell nP \pm d\theta = \left[\frac{-J\sin\theta}{r} - \frac{F_V}{\gamma P M^2}\right]\frac{\sin\mu}{\cos(\theta \pm \mu)}\, dx \tag{13}$$

In the above relations, μ is the Mach angle ($\sin\mu = 1/M$) and F_V is the viscous source term defined by

$$F_V = S_Q - (\gamma - 1)M^2\left[\frac{S_H}{Q} - S_Q\right] \tag{14}$$

where

$$S_Q = \frac{\cos\theta}{r^J}\frac{\partial}{\partial r}\left(r^J \mu_t \frac{\partial U}{\partial r}\right)$$

$$S_H = \frac{\cos\theta}{r^J}\frac{\partial}{\partial r}\left(\frac{r^J \mu_t}{\sigma_H}\frac{\partial H}{\partial r}\right) + \frac{\partial}{\partial r}\left(\frac{r^J \mu_t (\sigma_H - 1)}{\sigma_H}\frac{\partial}{\partial r}\left(\frac{U^2}{2}\right)\right)$$

and Q is the total flow velocity [$Q = (U^2 + V^2)^{1/2}$].

Computational Procedures

Grid Distribution and Jet Boundary Growth

Grid points are distributed evenly between the lower and upper boundaries of the domain being calculated. For significantly underexpanded jets, the multiple mapped domain approach utilized in the inviscid SCIPPY model[11] is employed to resolve the strong gradients in the nozzle lip region. For moderately underexpanded jets, a single mapped domain extending from the jet axis to the outer edge of the jet mixing layer suffices, as exhibited in Fig. 4. The position of the jet mixing layer edge is determined via the stepwise integration of the differential equation

$$\frac{dr_u}{dx} = \tan\tilde{\theta} + \frac{Cr_u}{f_L}\left(\frac{\partial f}{\partial r}\right)_u \tag{15}$$

which combines inviscid slipstream and viscous entrainment-type relations in an additive fashion (i.e., in the inviscid limit, the jet outer edge would be the plume slipstream surface defined by $dr_u/dx = \tan\theta$; for constant pressure mixing, the jet growth would be related to the gradients $\partial f/\partial r$, at the outer edge). For supersonic external flows, the angle $\tilde{\theta}$ is taken at the jet outer edge; for quiescent or subsonic external flow, $\tilde{\theta}$ is evaluated at the jet sonic line (Fig. 1) since the negative, entrainment-induced flow angles can become quite large as the external velocity approaches zero and thus do not represent the effective viscous dividing streamline angle. The variables f monitored at the jet outer edge to control viscous jet growth are the velocity U and species parameter ϕ (the maximum of these two gradients is utilized).

To obtain detailed grid resolution in the thin near-field shear layer, a grid embedding option can be utilized (Fig. 4). The "coarse" grid points $I = 1,2,\ldots,I_{\max}$ are distributed equally across the plume [$\Delta\eta = 1/(I_{\max} - 1)$]. The fine grid

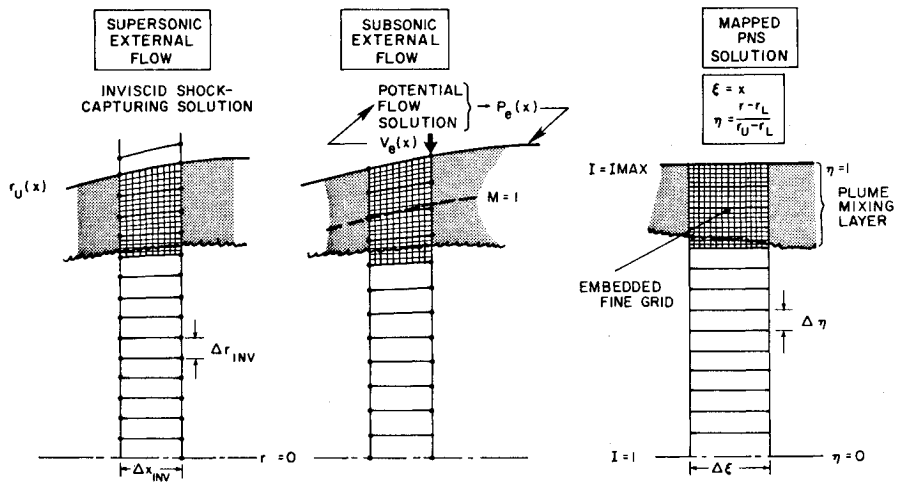

Fig. 4 Mapped grid distribution with embedded fine grid in thin shear layer region.

region is initiated at the coarse grid point $\tilde{I}$ sitting one grid interval below the shear layer, as ascertained by monitoring the species parameter profile. The coarse grid intervals, $\Delta\eta$, are subdivided into fine grid intervals, $\Delta\tilde{\eta}$, such that $\Delta\tilde{\eta}/\Delta\eta = 2^n$, where n varies in accordance with the relative width of the plume shear layer to the overall plume width. The coarse grid solution is advanced a step, $\Delta\xi$, for grid points $I=1$ to $\tilde{I}$, while the fine grid region above $\tilde{I}$ is integrated to $\xi+\Delta\xi$ using smaller steps, $\Delta\tilde{\xi}$, with the "inviscid" boundary conditions along $\tilde{I}$ fixed by the coarse grid solution. The details of this grid-embedding procedure are provided in Ref. 26.

Numerical Algorithm

A generalized two-step algorithm is utilized throughout the jet to advance the solution from ξ to $\xi+\Delta\xi$ for equally spaced grid intervals, $\Delta\eta$. The predictor/corrector sequence utilized is listed below.

Predictor step:

$$\tilde{E}_I = E_I^K - \frac{\Delta\xi}{\Delta\eta}\{(1-e)F_{I+1} - (1-2e)F_I - eF_{I-1} - G_I\Delta\xi\} + \frac{\Delta\xi b^2}{r_I^J \Delta\eta^2}\{A^+(f_{I+1}-f_I) - A^-(f_I - f_{I-1})\} \tag{16a}$$

Corrector step:

$$E_I^{K+1} = \frac{1}{2}\left[E_I^K + \tilde{E}_I - \frac{\Delta\xi}{\Delta\eta}\{e\tilde{F}_{I+1} + (1-2\epsilon)\tilde{F}_I + (e-1)\tilde{F}_{I-1}\} - \tilde{G}_I\Delta\xi + \frac{\Delta\xi\tilde{b}^2}{\tilde{r}_I^J\Delta\eta^2}\{\tilde{A}^+(\tilde{f}_{I+1}-\tilde{f}_I) - \tilde{A}^-(\tilde{f}_I - \tilde{f}_{I-1})\}\right] \tag{16b}$$

The term $A^{\pm}$ is given by

$$A^{\pm} = \frac{1}{2}\left[\left(\frac{r^J\mu_t}{\sigma_f}\right)_I + \left(\frac{r^J\mu_t}{\sigma_f}\right)_{I\pm1}\right]$$

and e is an upwind/alternating one-sided convective difference parameter whose operation differs in different flow regions, as will be described below.

Supersonic Marching

In supersonic viscous or inviscid flow regions, the convective difference parameter e in the above difference equations is varied between zero and one in the predictor and corrector steps to provide one-sided, alternating differences for shock capturing. The resultant algorithm is the steady flow equivalent of the explicit MacCormack algorithm.[33] The "e" sequence is alternated at subsequent marching steps to yield a nonpreferential treatment of wave propagation. A conventional supersonic decode procedure[11] is used to obtain the variables P, ρ, U, V, H, ϕ, k, and ϵ from the conservation arrays at the end of the predictor and corrector steps.

In a number of applications of the supersonic algorithm, oscillatory behavior of the scalar variables (H, ϕ, k, and/or ϵ) occurred in situations where the mapped grid was significantly skewed with respect to the streamline directions and radial gradients of the scalar variables were large. In parabolic problems, this unstable behavior is remedied by the use of an upwind convective operator. To provide this remedy in a viscous shock-capturing algorithm, the convective difference operator for the scalar components of the F vector array can be split into upwind and alternating one-sided difference components as follows:

$$\frac{\partial F^*}{\partial\eta} = \underset{\text{alternating}}{\alpha\frac{\partial}{\partial\eta}(\rho V)} + \underset{\text{upwind}}{\rho V\frac{\partial\alpha}{\partial\eta}} \tag{17}$$

where

$$\alpha = [H, \phi, k, \epsilon]^T$$

and F^* represents the scalar elements of the F vector array. With this splitting, the following convective difference expressions are utilized in the predictor and corrector steps.

Predictor step:

$$\frac{\partial F^*}{\partial\eta} = \frac{1}{\Delta\eta}[\alpha_I\{(1-e)(\rho V)_{I+1} - (1-2e)(\rho V)_I - e(\rho V)_{I-1}\} + (\rho V)_I^K\{(1-e^*)\alpha_{I+1} - (1-2e^*)\alpha_I - e^*\alpha_{I-1}\}] \tag{18a}$$

Corrector step:

$$\frac{\partial\tilde{F}^*}{\partial\eta} = \frac{1}{\Delta\eta}[\tilde{\alpha}_I\{e(\rho\tilde{V})_{I+1} + (1-2e)(\rho\tilde{V})_I + (e-1)(\rho\tilde{V})_{I-1}\} + (\tilde{\rho}\tilde{V})_I\{e^*\tilde{\alpha}_{I+1} + (1-2e^*)\tilde{\alpha}_I + (e^*-1)\tilde{\alpha}_{I-1}\}] \tag{18b}$$

The parameter e is the standard alternating difference parameter, whereas e^* is the upwind difference parameter defined (in both the predictor and corrector steps) by

$$e^* = 1 \quad \text{if } V/U \geq a/b$$
$$= 0 \quad \text{if } V/U < a/b$$

where a and b are the mapping parameters given by Eq. (11). For the continuity and momentum equations, the standard alternating-difference MacCormack algorithm is utilized with no splitting. The splitting of the scalar components of the F vector array has no effect on the shock-capturing characteristics of the algorithm since the scalar variables *all* change continuously across the shock waves.

It should be noted that a distinction is made between supersonic viscous and inviscid flow regions as ascertained by monitoring the position of the inner mixing layer profile (via inspection of the ϕ species parameter array) which "floats" across the grid points in working its way down to the jet axis. Below the inner mixing layer boundary, the inviscid (hyperbolic) limit of the PNS equations applies which is achieved via setting the turbulent viscosity to zero for all grid points in this region. While the full PNS equations could be integrated across the entire jet, the representation of turbulence properties in the inviscid core using a high Reynolds number, two-equation turbulence model can pose numerical problems since the parabolized turbulence equations are not representative of the turbulence processes occurring (i.e., the requisite terms needed to represent core turbulence, the production of turbulence behind shocks and subsequent dissipation, etc., are not included in the parabolized turbulence model). Hence, it is most expeditious to eliminate the solution of the turbulence model equations in nonmixing regions rather than to solve an inappropriate system of equations.

Subsonic Marching

In subsonic regions of the jet (Fig. 1), the equations are rendered parabolic or partially parabolic (parabolic in the streamwise direction, quasielliptic in the transverse direction) using the pressure-splitting approximation popularized for mixing problems by Patankar and Spalding.[12] In this approach, the streamwise pressure gradient, $\partial P/\partial X$, is imposed permitting a parabolic spatial integration of the axial momentum equation (plus the scalar equations for H, ϕ, k, and, ϵ/W). The transverse pressure and radial velocity variations are obtained via the a posteriori solution of the continuity and normal momentum equations. The ap-

plications of this approach in the framework of the numerical algorithm given by Eq. (16) are summarized below.

1) The pressure field at the new integration step, $\xi+\Delta\xi$, is approximated by integration of the following relation along each mapped grid point, $\eta=$const,

$$\frac{\partial P}{\partial \xi}=\frac{\overline{\partial P}}{\partial X}+a(\xi,\eta)\frac{\partial P}{\partial \eta} \tag{19}$$

where $\overline{\partial P/\partial X}$ is the imposed streamwise gradient, a the mapping parameter, and $\partial P/\partial\eta$ evaluated at ξ in the predictor step and $\xi+\Delta\xi$ in the corrector step.

2) A predictor/corrector "parabolic" integration of the conservation equations is performed utilizing the *upwind* form of the convective difference parameter, e, in Eqs. (16).

3) At the end of the predictor and corrector steps, a "subsonic decode procedure" is performed which takes cognizance of the imposed streamwise pressure gradient. With P^* designating the pressure at $\xi+\Delta\xi$ determined via Eq. (19), the following decode relations are utilized:

$$U=(e_u-P^*)/e_\rho \tag{20a}$$

$$V^*=e_v/e_\rho \tag{20b}$$

$$H=e_H/e_\rho \tag{20c}$$

and (for a perfect gas), the density ρ^* is evaluated from the state equation

$$\rho^*=\frac{\gamma P^*}{(\gamma-1)\left[H-\tfrac{1}{2}(U^2+V^{*2})\right]} \tag{21}$$

Note that the E conservation array of Eqs. (16) must be reconstructed upon completion of both the predictor and corrector steps since the subsonic integration procedure is not fully conservative [i.e., ρ^* determined from Eq. (21) is not identical to e_ρ/U].

4) Revised values of P^*, V^*, and ρ^* are determined after completion of the predictor/corrector parabolic sequence above via the coupled solution of the continuity, normal momentum, and state equations. The cross-flow integration can be performed using the iterative, linearized procedure of Patankar and Spalding,[12] the uncoupled, iterative procedure of Mahgoub and Bradshaw,[23] or the noniterative fully coupled method of Dash et al.[25,34] For the free jet problems described herein (i.e., moderately underexpanded jets into still air), the pressure variations across the subsonic portion of the jet and Mach disk mixing layers are quite small and can be neglected. Then, a simplified cross-flow integration is performed with P^* held fixed at the edge value and ρ^* and V^* determined from the linearized solution of the continuity and state equations as described in Ref. 26.

Axial Step Size Constraints

The present subsonic/supersonic marching procedure is fully explicit and thus the axial step size $\Delta\xi$ is limited by well-known hyperbolic and parabolic stability constraints. In supersonic inviscid regions, the hyperbolic CFL constraint is satisfied in a nonlinear fashion via locating the intersection of the $\lambda^\pm$ characteristics with the mapped coordinate lines, $\eta=$const, at each grid point; and, determining the minimum intersection distance. This is achieved utilizing the relation

$$(\Delta\xi_I^{\pm})_{\text{hyp}}\le\left[\frac{\pm b\Delta\eta}{\tan\omega_I-\tan(\theta\pm\mu)_{I\pm1}}\right]_{\min} \tag{22}$$

where ω designates the inclination of the mapped grid lines, $\eta=$const, with respect to the jet axis. In subsonic viscous regions, the standard explicit parabolic stability constraint listed below is applied.

$$(\Delta\xi_I)_{\text{par}}\le\left[\frac{0.5\rho U\sigma_{\min}b^2\Delta\eta^2}{\mu_t}\right]_I \tag{23}$$

In viscous supersonic regions, the hyperbolic and parabolic constraints are combined in the fashion introduced by Cheng[35] in the explicit, time-dependent solution of the N-S equations, and proven effective in numerous hyperbolic/parabolic steady and nonsteady flow applications. The combined constraint is

$$(\Delta\xi_I)_{\text{hyp/par}}=\left[\frac{1}{\frac{1}{\Delta\xi_{\text{hyp}}}+\frac{1}{\Delta\xi_{\text{par}}}}\right] \tag{24}$$

Direct Coupling of Jet and External Flow Solutions

Referring to Fig. 4, the jet and external flow solutions are "directly coupled" at the outer edge of the jet mixing layer, $r_u(x)$ (which corresponds to $\eta=1$ in the mapped domain). For supersonic external streams, the external flow solution is obtained by a concurrent spatial integration of the inviscid shock-capturing equations in a second mapped domain extending from $r_u(x)$ to the fitted plume bow shock (Fig. 1). Alternatively, a reasonable approximation of the supersonic external flow can be obtained via the application of simple pressure/flow deflection relations along $r_u(x)$ (see Ref. 11).

For a quiescent external stream, the pressure is stipulated to be the ambient value along $r_u(x)$ and a nominal nonzero value of the freestream velocity is assigned (i.e., 1/100th of the jet value). The coupling of the jet and quiescent external flow requires matching the subsonic and supersonic solutions in the vicinity of the jet mixing layer sonic line as schematized in Fig. 5. The matching occurs at the grid point I^* which sits below the sonic line. If the pressure variation across the

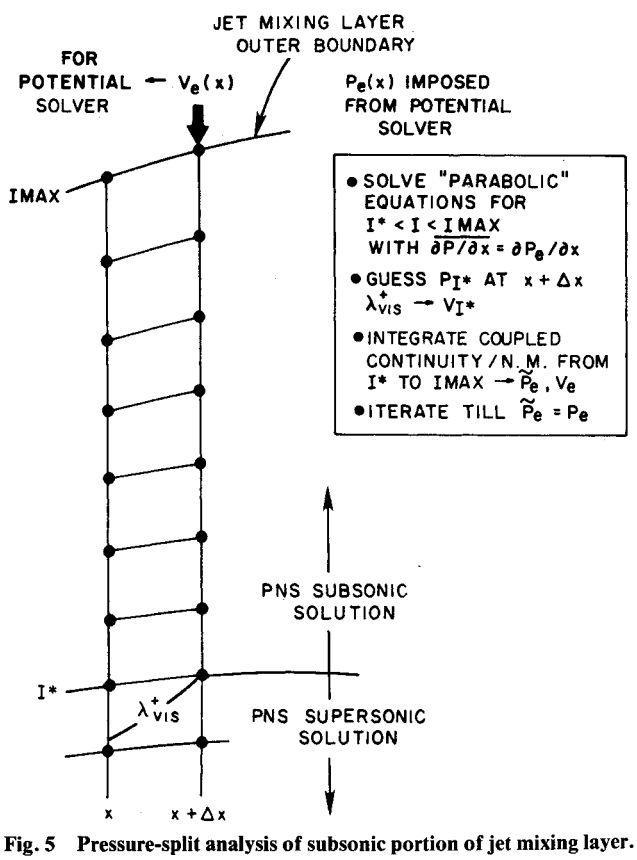

Fig. 5 Pressure-split analysis of subsonic portion of jet mixing layer.

subsonic portion of the jet is neglected, the ambient pressure is imposed at the I^* point and the flow angle θ^* at I^* is ascertained using the viscous-characteristic compatibility relation of Eq. (13) along the λ^+ characteristic [Eq. (12)] depicted in Fig. 5. The numerics involved in the predictor/corrector characteristic solution are enumerated in Ref. 26. Supersonic grid points below I^* are evaluated using the supersonic variant of the matching algorithm. Subsonic grid points above I^* are evaluated with $\partial P/\partial X$ set equal to zero in the pressure-splitting approximation, and, the continuity equation is solved via upward integration from the I^* point where V^* is known from the characteristic solution. To account for pressure variations across the subsonic region, a stepwise iterative procedure is performed whereby a value of P^* (at I^*) is assumed, the full cross-flow integration is performed yielding edge values of P_E and V_E, and P^* is varied until the outer boundary condition, $P_E = P_\infty$, is satisfied. This iterative sequence is summarized in Fig. 5.

The quiescent external flow solution described above represents a first approximation of the interactive jet flowfield and does not account for the perturbation effects of jet entrainment on the external flow. These effects can be accounted for by solving the potential flow about an effective body defined by $r_u(x)$ with the transpiration boundary condition $\phi_n = V_E(x)$, where V_E is the predicted entrainment (radial) velocity along $r_u(x)$. This yields the induced pressure variation, $P_E(x)$, and corresponding streamwise velocity distribution, $U_E(x)$, to be imposed as outer boundary conditions for a subsequent jet sweep. The entrainment-induced external flow perturbations have a small influence on the jet shock structure for the first several shock cells but appear to have a noticeable effect on the pressure variations in the last several shock cells where the pressure amplitudes are weak (see Ref. 20).

Iterative coupling of the jet and subsonic external flow solutions parallels the interactive procedure described above. The jet boundary conditions, $P_E(x)$ and $U_E(x)$, along $r_u(x)$ are determined from the potential external flow solution, and the external flow solution is solved with a transpiration boundary condition corresponding to the entrainment velocity, $V_E(x)$. The jet boundary, $r_u(x)$, can be set to encompass the full viscous/inviscid jet and remain invariant through the jet/potential flow iterative cycles if the growth constant C in Eq. (15) is set equal to a value of about 10 in the first jet sweep [this yields a buffer region of several grid points between the physical jet edge and $r_u(x)$, whereas a value of $C \sim 1$ places the physical and computational boundaries in close proximity]. Subsequent jet sweeps are performed with the $r_u(x)$ variation established in the first sweep imposed. For transonic external streams with large pressure gradients, the pressure-splitting approximation, $\partial P/\partial X = \partial P_E/\partial X$, may be inadequate (i.e., significant radial variations of the streamwise pressure gradient can occur across the subsonic portion of the mixing layer). A global pressure iteration, localized to the region of large gradients, can be performed to improve the solution following the approach of Mahgoub and Bradshaw[23] in the manner described in Ref. 25. The "direct" jet/potential flow coupling approach described above is still under development, and applications to jets in subsonic/transonic external streams will be described in a future article.

Analysis of Mach Disk Mixing Regions

While the Mach disk problem has previously been treated from an inviscid point of view,[11,36,37] it has been exhibited both analytically[38,39] and experimentally[40] that turbulent mixing processes initiated along the Mach disk slipstream (Fig. 6) can contribute strongly to the acceleration of the subsonic flow behind the disk to supersonic velocities.

Referring to Fig. 6, the mixing process that occurs between the inner subsonic flow that has traversed the Mach disk and the outer supersonic flow has strong wake-like characteristics (viz., outer to inner ρU ratios exceed 10 and can exceed 50 for highly underexpanded exhausts). The entrainment process displaces the outer streamlines inward at a very rapid rate for the first few Mach disk radii producing strong interactive effects. A simple procedure based on the "porous-sting" approach of Dash et al.[21] for the two-phase Mach disk problem has been developed for treating this interactive mixing process. This simplified approach utilizes a pressure-split "sublayer approximation" to eliminate elliptic (saddle-point) behavior in the marching process. This approach is applicable for smaller radius disks where the extent of the embedded subsonic zone behind the disk is small compared to the jet width and for which the turbulent mixing process dominates the acceleration of the inner flow to the supersonic velocities. The results obtained are in qualitative accord with the experimental observations of Back and Cuffel.[40] The basic features of the Mach disk methodology are summarized below.

The disk position is located using the "sting" triple-point criterion discussed in Ref. 11 which, for smaller radius disks, is analogous to the earlier criterion of Bowyer et al.,[41] and has been demonstrated to properly locate small radius disk positions in a number of earlier comparative studies. A formal shock-fitting procedure is utilized in the calculation of the triple-point solution.[11] If the sting criterion has not been satisfied by the time the downrunning shock reaches the jet axis, the shock is regularly reflected. In cases where a disk is dropped, a grid point, sitting several grid points above the viscous sonic line (Fig. 6), serves as the matching point between the inner subsonic and outer supersonic flows. A specified matching Mach number (typically 1.1-1.5) delineates the grid point at which inner/outer matching is performed. The grid points *above* the matching point are integrated using the supersonic PNS algorithm, while the grid points below the matching point are integrated using a simplified variant of the subsonic PNS algorithm with the pressure split using a sublayer-type approximation. The index of the matching point changes from step to step in accordance with the monitored spatial variation of the sonic line. When the sonic line reaches the jet axis, the supersonic PNS algorithm is employed throughout the Mach disk mixing region and inner/outer matching is no longer required.

The following steps are entailed in the inner/outer Mach disk matching:

1) A value of the pressue gradient, $\partial P/\partial x$, at the matching point $I = I^*$ is assumed.

2) The inner pressure field is split with the *streamwise pressure gradient* term in the axial momentum equation damped in accordance with the following heuristic sublayer

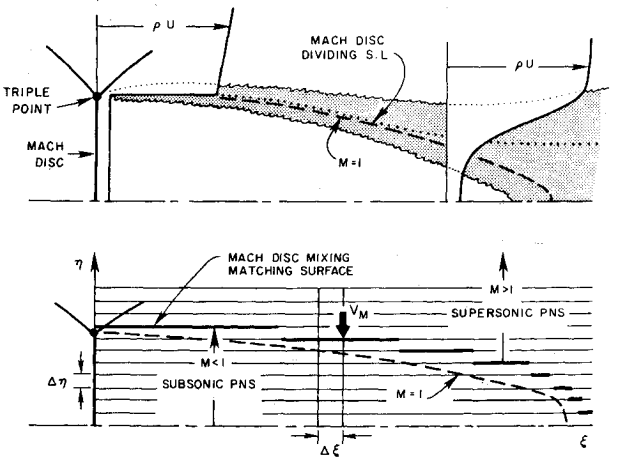

Fig. 6 Characteristic features of Mach disk mixing region and subsonic/supersonic matching surface.

approximation:

$$\left(\frac{\partial P}{\partial x}\right)_I = \left(\frac{\partial P}{\partial x}\right)_{I^*} \frac{(M_I^2-1)}{(M_{I^*}^2-1)} \quad \text{for } M_I > 1 \tag{25a}$$

$$\left(\frac{\partial P}{\partial x}\right)_I = 0 \quad \text{for } M_I < 1 \tag{25b}$$

and the pressure, itself, given by

$$P_I = P_{I^*} + \left(\frac{\partial P}{\partial x}\right)_{I^*} \Delta x$$

(i.e., the pressure is uniform across the mixing region but the pressure gradient is variable in the transonic portion and completely suppressed in the subsonic region).

3) The inner grid points are integrated using the subsonic parabolic algorithm yielding the radial velocity at the matching surface V^* and hence the "inner" flow deflection angle θ^*.

4) The "inner" value of θ^* is compared with an "outer" value determined using the downrunning viscous-characteristic compatibility relation along the λ^- characteristic passing through the matching point I^*. Steps 2-4 are repeated varying the assumed pressure gradient until the inner and outer values of θ^* agree to within a prescribed tolerance.

The treatment of larger disks entails accounting for elliptic upstream influence effects using iterative methodology in conjunction with a downstream saddle-point type viscous throat constraint[42] analogous to the minimum area throat constraint utilized in the Abbett inviscid Mach disk approach[36] and incorporated in earlier inviscid versions of the SCIPPY model.[2,11] The streamwise iterative PNS approach required to treat larger radius disks appears to be a straightforward extension of the present small disk methodology utilizing the automated iterative approach formulated for dealing with this saddle-point-type problem in the inviscid limit.[2,11]

Concluding Remarks

A new approach for analyzing interactive phenomena occurring in supersonic jet mixing problems has been described based on the spatial integration of the parabolized Navier-Stokes jet mixing equations. This approach combines shock-capturing methodology for the analysis of supersonic viscous or inviscid regions with pressure-splitting methodology for the analysis of subsonic viscous regions, and, provides for the formal coupling of subsonic and supersonic jet regions in the vicinity of viscous sonic lines utilizing a viscous-characteristic coupling procedure. The formation of Mach disks in the jet and the analysis of the interactive turbulent mixing process occurring behind Mach disks are included in the methodology developed. Jet and Mach disk mixing processes are analyzed utilizing two-equation turbulence models.

The PNS equations are integrated in a mapped rectangular domain which encloses the full viscous/inviscid jet. The jet boundary growth is controlled by a differential equation which combines plume expansion and entrainment effects in an additive fashion. Via this mapping, the interactive coupling of the viscous/inviscid jet and external flow solutions is performed utilizing a direct-coupling technique along the outer jet boundary. For supersonic external flows, the PNS jet and external flow solutions can be solved concurrently. For subsonic external flows, the coupling is interactive: the jet solution is solved with the pressure and axial velocity variation imposed along the matching surface and yields the entrainment (radial) velocity variation; the external potential flow solution is solved over the matching surface with a transpiration boundary condition corresponding to the jet entrainment velocity.

In Part II of this paper,[43] applications of this approach to a number of jet mixing problems are presented exhibiting some of the fundamental interactive phenomena occurring in supersonic mixing problems, and, the ability of the methodology developed to analyze them. This approach is presently operational for jets exhausting into supersonic or quiescent external streams. The iterative coupling of this PNS jet solution with a potential external flow solution, required to analyze jets exhausting into subsonic/transonic external streams is now in progress and will be described in a future publication. A noniterative subsonic cross-flow integration procedure developed for curved wall jet applications[25,34] will be utilized in performing this coupling to account for pressure variations across the subsonic portion of the jet mixing layer.

A computer code, SCIPVIS,[19] has been developed which employs this methodology to predict the multiple-cell, decaying shock structure in axisymmetric jets for applications to shock-noise predictions.[20] A detailed assessment of this code utilizing the experimental data of Seiner and Norum[9] is given in Ref. 20 which highlights the sensitivity of the jet pressure field to the turbulence modeling representations employed.[19] Progress toward incorporating this PNS methodology into the JANNAF Standard Plume Flowfield Model for the analysis of chemically reacting, two-phase rocket exhaust plumes is discussed in Ref. 22. A three-dimensional version of the SCIPVIS code recently has been made operational for the analysis of imperfectly expanded jets issuing from rectangular nozzles which will be discussed in a forthcoming publication.[44]

Acknowledgments

This work was supported by the Propulsion Aerodynamics and Aeroacoustics Branches of the NASA Langley Research Center under Contract NAS1-16535. The cognizant technical monitors were Dr. R. G. Wilmoth of the Propulsion Aerodynamics Branch and Dr. J. M. Seiner of the Aeroacoustics Branch.

References

[1] Dash, S. M. and Pergament, H. S., "A Computational Model for the Prediction of Jet Entrainment in the Vicinity of Nozzle Boattails (The BOAT Code)," NASA CR-3075, Dec. 1978.

[2] Dash, S. M., Pergament, H. S., and Thorpe, R. D., "Computational Models for the Viscous/Inviscid Analysis of Jet Aircraft Exhaust Plumes," NASA CR-3289, May 1980.

[3] Dash, S. M., "Computational Techniques for the Viscous/Inviscid Analysis of Exhaust Plume Flowfields," *Advances in Computer Methods for Partial Differential Equations, IV*, edited by R. Vichnevetsky and R. S. Stepleman, IMACS, Rutgers Univ., New Brunswick, N. J., 1981, pp. 206-216.

[4] Dash, S. M. and Pergament, H. S., "The JANNAF Standard Plume Flowfield Model (SPF)," U. S. Army Missile Command, TR RD-CR-82-9, April 1981.

[5] Dash, S. M., Pergament, H. S., and Wolf, D. E., "Computation of Viscous/Inviscid Interactions in Exhaust Plume Flowfield, Part I: Overlaid and Fully-Coupled Methodology," *Proceedings of the Symposium on Rocket/Plume Fluid Dynamic Interactions, Volume I—Base Flows*, Huntsville, Ala., U.S. Army Research Office Fluid Dynamics Laboratories, Rept. 83-101, April 1983.

[6] Dash, S. M., Wilmoth, R. G., and Pergament, H. S., "An Overlaid Viscous/Inviscid Model for the Prediction of Nearfield Jet Entrainment," *AIAA Journal*, Vol. 17, Sept. 1979, pp. 950-958.

[7] Dash, S. M., Pearce, B. E., Pergament, H. S., and Fishburne, E. S., "Prediction of Rocket Plume Flowfields for IR Signatures Studies," *Journal of Spacecraft and Rockets*, Vol. 17, May-June 1980, pp. 190-199.

[8] Wilmoth, R. G., "RAXJET: A Computer Program for Predicting Transonic Axisymmetric Flow Over Nozzle Afterbodies with Supersonic Jet Exhausts," NASA TM 83235, Feb. 1982.

[9] Seiner, J. M. and Norum, T. D., "Experiments of Shock Associated Noise on Supersonic Jets," AIAA Paper 79-1526, July 1979.

[10] Wilmoth, R. G. and Dash, S. M., "A Viscous-Inviscid Interaction Model of Jet Entrainment," *Computation of Viscous-Inviscid Interactions*, AGARD CP-291, 1981, pp. 13.1-13.15.

[11] Dash, S. M. and Thorpe, R. D., "Shock-Capturing Model for One- and Two-Phase Supersonic Exhaust Flow," *AIAA Journal*, Vol. 19, July 1981, pp. 842-851.

[12] Patankar, S. V. and Spalding, D. B., "A Calculational Procedure for Heat, Mass, and Momentum Transfer in Three-Dimensional Parabolic Flows," *International Journal of Heat and Mass Transfer*, Vol. 15, Oct. 1972, pp. 1787-1806.

[13] Ferri, A. and Dash, S. M., "Viscous Flow at High Mach Numbers with Pressure Gradients," *Viscous Interaction Phenomena in Supersonic and Hypersonic Flow*, University of Dayton Press, Dayton, Ohio, 1970, pp. 271-318.

[14] McDonald, H. and Briley, W. R., "Three-Dimensional Supersonic Flow of Viscous or Inviscid Gas," *Journal of Computational Physics*, Vol. 19, Oct. 1975, pp. 150-178.

[15] Jenkins, R. V., "An Improved Viscous-Characteristics Analysis Program," NASA TP 1289, Nov. 1978.

[16] Markatos, N. C., Spalding, D. B., and Tatchell, D. G., "Combustion of Hydrogen Injected into a Supersonic Airstream (The SHIP Computer Program)," NASA CR-2802, April 1977.

[17] Elgobashi, S. and Spalding, D. B., "Equilibrium Chemical Reaction of Supersonic Hydrogen-Air Jets (The ALMA Computer Program)," NASA CR-2725, Jan. 1977.

[18] Dash, S. M. and Wolf, D. E., "Development of Fully-Coupled Viscous/Inviscid Technology for the Analysis of Exhaust Plume Flowfields," *JANNAF 13th Plume Technology Meeting*, CPIA Pub. 357, Vol. 1, April 1982, pp. 115-182.

[19] Dash, S. M., and Wolf, D. E., "Shock-Capturing Parabolized Navier-Stokes Model (SCIPVIS) for the Analysis of Turbulent Underexpanded Jets," AIAA Paper 83-0704, April 1983.

[20] Seiner, J. M., Dash, S. M., and Wolf, D. E., "Shock Noise Features Using the SCIPVIS Code," AIAA Paper 83-0705, April 1983.

[21] Dash, S. M., Beddini, R. A., Wolf, D. E., and Pergament, H. S., "Analysis of Two-Phase Flow Processes in Rocket Exhaust Plumes," AIAA Paper 83-0248, Jan. 1983.

[22] Dash, S. M., Wolf, D. E., and Pergament H. S., "Overlaid and Fully-Coupled Two-Phase Flow Versions of JANNAF Standard Plume Flowfield Model," *JANNAF 14th Plume Technology Meeting*, CPIA Pub. 384, Vol. II, Nov. 1983, pp. 169-225.

[23] Mahgoub, H. E. H. and Bradshaw, P., "Calculation of Turbulent-Inviscid Flow Interactions with Large Normal Pressure Gradients," *AIAA Journal*, Vol. 17, Oct. 1979, pp. 1025-1029.

[24] Khosla, P. K. and Rubin, S. G., "A Composite Velocity for the Compressible Navier-Stokes Equations," AIAA Paper 82-0099, Jan. 1982.

[25] Dash, S. M., Beddini, R. A., Wolf, D. E., and Sinha, N., "Viscous/Inviscid Analysis of Curved Sub- or Supersonic Wall Jets," AIAA Paper 83-1679, July 1983.

[26] Dash, S. M. and Wolf, D. E., "Fully-Coupled Analysis of Jet Mixing Problems, Part I: Shock-Capturing Model, SCIPVIS," NASA CR 3761, Jan. 1984.

[27] Launder, B. E., Morse, A., Spalding, D. B., and Rodi, W., "Prediction of Free Shear Flows: A Comparison of Six Turbulence Models," *Free Turbulent Shear Flows*, Vol. 1, NASA SP-321, 1972, pp. 361-426.

[28] Dash, S. M., Weilerstein, G., and Vaglio-Laurin, R., "Compressibility Effects in Free Turbulent Shear Flows," AFOSR-TR-75-1436, Aug. 1975.

[29] Jensen, D. E. and Wilson, A.S., "Prediction of Rocket Exhaust Flame Properties," *Combustion and Flame*, Vol. 25, 1975, pp. 43-55.

[30] Spalding, D. B., "Concentration Fluctuations in a Round Turbulent Free Jet," *Chemical Engineering Science*, Vol. 26, 1971, pp. 95-107.

[31] Pergament, H. S., "Assessment and Recommendation of Two-Equation Turbulence Models for Rocket and Aircraft Plume Flowfield Predictions," NWC TP 6364, July 1982; also, *JANNAF 13th Plume Technology Meeting*, CPIA Pub. 357, Vol. II, April 1982, pp. 73-126.

[32] Padova, C., "Non-Reacting Turbulent Mixing Experiments," Calspan Advanced Technology Center, Buffalo, N. Y., Rept. 6632-A-3, Jan. 1983.

[33] MacCormack, R. W., "The Effects of Viscosity in Hypervelocity Impact Cratering," AIAA Paper 69-354, 1969.

[34] Dash, S. M. and Sinha, N., "Noniterative Cross-Flow Integration Procedure for the Pressure-Split Analysis of Two-Dimensional, Subsonic Mixing Layer Problems," to be published, *AIAA Journal*.

[35] Cheng, S. I., "Numerical Integration of Navier-Stokes Equations," *AIAA Journal*, Vol. 8, Dec. 1970, pp. 2115-2123.

[36] Abbett, M. J., "Mach Disc in Underexpanded Exhaust Plumes," *AIAA Journal*, Vol. 9, March 1971, pp. 512-514.

[37] Fox, J., "On the Structure of Jet Plumes," *AIAA Journal*, Vol. 12, Jan. 1974, pp. 105-107.

[38] Dash, S. M., and Pergament, H. S., "A Computational System for the Analysis of Mixing/Chemical/Shock Processes in Supersonic Internal and Exhaust Plume Flowfields," AIAA Paper 80-1255, 1980.

[39] Hasen, G. A., "Navier-Stokes Solutions for an Axisymmetric Nozzle in a Supersonic External Stream," AFWAL TR-81-3161, April 1981.

[40] Back, L. H. and Cuffel, R. B., "Viscous Slipstream Flow Downstream of a Centerline Mach Reflection," *AIAA Journal*, Vol. 9, Oct. 1971, pp. 2107-2109.

[41] Bowyer, J., D'Attorre, L., and Yoshihara, H., "Transonic Aspects of Hypervelocity Rocket Plumes," *Supersonic Flow, Chemical Processes, and Radiative Transfer*, Pergamon Press, Ltd., London, 1964, pp. 203-209.

[42] Weinbaum, S. and Garvine, R. W., "On the Two-Dimensional Viscous Counter-part of the One-Dimensional Sonic Throat," *Journal of Fluid Mechanics*, Vol. 39, 1969, pp. 55-85.

[43] Dash, S. M. and Wolf, D. E., "Interactive Phenomena in Supersonic Jet Mixing Problems, Part II: Numerical Studies," to be published, *AIAA Journal*.

[44] Dash, S. M., Wolf, D. E., and Sinha, N., "Parabolized Navier-Stokes Analysis of Three-Dimensional Supersonic and Subsonic Jet Mixing Problems," AIAA Paper No. 84-1525, June 1984.